University of Guilan

Caspian Journal of Intelligent and Mechatronic Systems

https://cjiams.guilan.ac.ir

Caspian Journal of INTELLIGENT and MECHATRONIC SYSTEM

Full Multibody Dynamic Model Predictive Control for Cooperative Transportation Using a Minimal Configuration of Two Nonholonomic Mobile Robots

Zahra Shirmohamadi [a], Hamed Kouhi [a,*], Behnam Miripour Fard [a], Esmaeil Salahshoor [b]

[a] Faculty of Mechanical Engineering, University of Guilan, Rasht, Iran.

[b] Department of Mechanical Engineering, Islamic Azad University of Izeh, Izeh, Iran

ARTICLE INFO

Article history:
Received May 24, 2026
Accepted July 24, 2026
Available online July 24, 2026

Keywords:
Cooperative transportation
Nonholonomic mobile robots
Full multibody dynamics
Contact maintenance constraints
Minimum robot configuration.

ABSTRACT

This paper presents a cooperative transportation strategy for a rigid body manipulated by only two nonholonomic mobile robots using a full multibody dynamic model predictive control (MPC) approach. Unlike existing methods that rely on quasi-static assumptions or simplified kinematic models, which neglect inertial effects, our formulation explicitly incorporates the complete coupled dynamics of the robot–object system, including inertial effects, nonholonomic constraints, and physical contact interactions. A centralized MPC scheme is developed to compute optimal control inputs while simultaneously enforcing three critical constraint sets: (1) actuator saturation limits, (2) nonholonomic motion constraints of differential-drive robots, and (3) explicit contact maintenance constraints that prevent robot detachment from the object. Numerical simulations demonstrate that the proposed framework successfully transports objects from arbitrary initial configurations (x=2 m, y=0.5m) to desired poses (x=2 m, y=0.5 m) while satisfying all system constraints. The settling time of approximately 4s is consistent with the system dynamics and actuator limits. The results confirm that only two nonholonomic robots are sufficient when using this advanced control methodology. This work establishes a foundation for dynamic-aware cooperative manipulation systems that bridge the gap between simplified kinematic approaches and physically realistic multibody implementations.

*. Corresponding author. Tel.: +98-13-33691065; Fax: +98-13-33691065.
E-mail address: hamed.koohi@guilan.ac.ir (H. Kouhi).

Doi:10.22124/cjiams.2026.33679.1001

1. Introduction

Cooperative robotics is an evolving domain that shows great potential for creating more resilient and adaptable robotic systems. Multi-robot systems provide flexible configurations and diverse functionalities, enabling them to adjust more readily to various environments and missions. They also enhance redundancy and improve coverage and throughput, which are particularly beneficial for operations in unfamiliar settings, such as search and rescue, exploration, and surveillance [1]. In this context, a cooperative robotic system is developed to autonomously transport objects that are too heavy or unwieldy for a single robot to handle alone. These multi-robot systems have numerous potential applications in everyday activities, including object transportation in manufacturing facilities, warehouses, construction sites, and other settings. Cooperative object transportation also necessitates a framework for multi-robot formation control to synchronize the movements of the robots within the group.

There are three common methods for transporting objects (1) *Grasping*: robots are physically attached to the object; (2) *Pushing-Only Strategy*: robots are not attached and transport is achieved by pushing; and (3) *Caging Strategy*: robots are distributed around the object to trap it [2]. The study by [3] is considered a pioneering work in collaborative transportation using a homogeneous group of simple robots that can only push objects. A performance study by [4] describes a group of three robots where one member acts as a watcher and the other two act as pushers. Another study by [5] considered a heterogeneous group of robots that collaborate to move a box by removing obstacles. For grasping strategies, [6] proposed an algorithm allowing a homogeneous group of robots to find an optimal arrangement around an object to be lifted and transported. A motion controller for a four-robot group is described by [7]. For caging strategies, [8] proposed an algorithm relying only on robots' ability to assess the direction of the object and the positions of neighbors.

Various methods have been employed for motion planning and control of robot teams, including MPC, artificial potential fields, and impedance control. In this work, MPC is utilized to determine control inputs while considering physical constraints such as actuator saturation. Recent research has compared formation control strategies for nonholonomic mobile robots in cooperative transport. [9] compared l-ψ control and Cartesian reference-based control, demonstrating that Cartesian control generally provides better results. [10] introduced a distributed MPC scheme for cooperative pushing of polygonal objects, where robots communicate only with immediate neighbors. [11] presented a decentralized control approach for nonholonomic robots transporting a load without rigid connections, utilizing physical interactions as the main means of information exchange. [12] proposed a leader-follower decentralized control system where the leader manipulates the object omnidirectionally and followers maintain constant relative positions using PI control. [13] developed a decentralized method for a homogeneous swarm of ant-like robots to collectively transport a palletized load, exploiting caster dynamics without direct communication.

Ref. [14] provided a comprehensive review of control strategies for large-scale material transport, classifying methods based on coordination architecture and mechanical platform design. Ref. [15] presented a design methodology for cooperative robots capable of manipulating and transporting payloads by tightening a payload between a set of mobile robots.

Nomenclature

Symbol	Description	Unit
L_1	half the width of the cube	m
L_2	half-length of the cube	m
w_1 , w_2	the minimum distances between the centers of the robot 1 and robot 2 relative to the centerlines of the cube	m
θ	cube yaw angle	rad
δ	the robot's body penetration into the cube	m
$\alpha_i\,(i=1,2)$	yaw angle of the robot i	rad
$R_i\,(i=1,2)$	the distance between the robot i center and the wheel	m
$\vec{F}_{Li}\,(i=1,2)$	the left wheel driving forces	N
$\vec{F}_{Ri}\,(i=1,2)$	the right wheel driving forces	N
$\vec{\lambda}_i\,(i=1,2)$	the lateral forces exerted from the ground to the wheels	N
$\vec{v}_i\,(i=1,2)$	the velocity of the robot center	m/s
$\vec{N}_i\,(i=1,2)$	contact forces between the robot i body and the cube	N
m	mass of the robots	kg
M	the mass of the cube	kg
(x_i, y_i)	Position components of the robot i center of mass	m
$(\dot{x}_i, \dot{y}_i)$	velocity components of the robot i center of mass	m/s
$(\ddot{x}_i, \ddot{y}_i)$	acceleration components of the robot i center of mass	m/s^2
(x_c, y_c)	Position components of the cube center of mass	m
$(\dot{x}_c, \dot{y}_c)$	velocity components of the cube center of mass	m/s
$(\ddot{x}_c, \ddot{y}_c)$	acceleration components of the cube center of mass	m/s^2
I	robots' moment of inertia around their centers	$Kg.m^2$
I_c	the cube moment of inertia around its center	$Kg.m^2$
K	stiffness coefficients of the cube	N/m
c	damping coefficients of the cube	Ns/m
ω_s	cube's angular velocity	rad/s

Ref. [16] proposed a motion planning method for cooperative transportation in a three-dimensional environment, dividing the planner into global path planning and local manipulation planning. [17] reviewed tracked locomotion systems for ground mobile robots, providing taxonomies relevant for designing robust mobile platforms. Ref. [18] introduced an occlusion-based cooperative transport strategy where robots push an object only where the direct line of sight to the goal is occluded, proving that any convex object can be transported without explicit communication. Ref. [19] presented a formation-based cooperative transportation approach using a virtual leader-follower strategy.

A critical challenge in cooperative transportation is determining the minimum number of robots required for stable and efficient object manipulation. While many studies employ three or more robots [7, 8, 10], only a few have investigated the feasibility of two-robot configurations.

Ref. [12] introduced a two-robot system where a follower robot uses fuzzy control for obstacle avoidance, but their kinematic model neglects inertial effects and contact dynamics. Ref. [13] demonstrated collective transport with a swarm of ant-like robots, yet their approach required many robots rather than a minimal configuration. [19] employed a virtual leader strategy but assumed quasi-static motion, limiting applicability during aggressive maneuvers. [20] recently proposed a dual-robot formation transport using improved DDPG navigation; however, their framework remains largely kinematic, does not incorporate multibody dynamics or robot–object contact forces, and lacks explicit constraint satisfaction guarantees. Similarly, [21] enhanced multi-robot manipulation with soft grippers and caging-based control, but their method does not address inertial effects or nonholonomic constraints, making it unsuitable for high-speed transport. In contrast to these studies, the present paper demonstrates that, for the simulated scenarios considered, two nonholonomic mobile robots are sufficient for cooperative transportation when a full multibody dynamic MPC framework is employed. Our formulation explicitly accounts for inertial coupling, contact forces, and nonholonomic constraints while enforcing actuator and contact maintenance constraints, features absent in the aforementioned two-robot approaches. This constitutes a significant advancement toward minimal-robot cooperative manipulation for dynamic environments. In contrast, the present paper derives a complete dynamic model of the coupled robot-object system and employs an MPC structure that enforces contact, actuator, and motion constraints simultaneously, providing greater physical fidelity for dynamic cooperative transportation scenarios.

A notable recent advancement is the work by [22], in which a cooperative transportation scheme for differential-drive mobile robots using distributed MPC and multibody dynamics representation is proposed for handling arbitrary polygonal objects. This demonstrates the growing recognition that multibody dynamics are essential for accounting for contact and nonholonomic constraints. Similarly, [23] integrated differentiable compliant contact models with MPC for online estimation of contact geometry, and [24] showed that interaction model estimation-based force-position optimization reduces impact forces by 50% in rigid-soft heterogeneous contact tasks.

In most studies on cooperative transportation, it is assumed that robots move slowly, thus the inertial effects of the agents are not considered in the mathematical modeling. Consequently, the dynamics model is not utilized during the controller design. Moreover, nonholonomic constraints of wheeled robots are included in the system modeling. This approach aligns with recent trends emphasizing the importance of dynamic modeling for achieving stable manipulation during aggressive maneuvers where inertial effects dominate [22, 23].

The remainder of the paper is organized as follows: The dynamic modeling of the two cooperative wheeled robots and the cube is presented in Section 2. In Section 3, the cooperative control strategy is introduced. The simulation results are provided in Section 4. The discussion is presented in Section 5. The paper is concluded in Section 6, followed by the references.

2. Dynamic modelling

The concept of cooperative transporting system is illustrated in Figure 1, where two autonomous wheeled robots are employed to move a large cube to a desired target area. Figure 1 shows a schematic of the system under study, which includes two cylindrical mobile robots that work together to move a cube in grasping strategy. In this figure, L_1 is half the width of the cube, L_2 is the half length of the cube, $\vec{d}_1$ and $\vec{d}_2$ are the position vectors of robots' centers relative to the center of the cube, w_1 and w_2 are the minimum distances between the centers of the robots relative to the centerlines of the cube as shown, θ is the cube yaw angle and δ is the robot's body penetration into the cube.

2.1 Derivation of the dynamic equations of the robots

In Figure 2 and Figure 3, the free-body diagrams of the two robots are shown. In these figures, $c_i\,(i=1,2)$ are the robots' centers of mass, $\alpha_i\,(i=1,2)$ represents the yaw angle of the robot, $R_i\,(i=1,2)$ are the distance between the robot center and the wheel, $\vec{F}_{Li}\,(i=1,2)$ are the left wheel driving forces, $\vec{F}_{Ri}\,(i=1,2)$ are the right wheel driving forces, $\vec{\lambda}_i\,(i=1,2)$ indicate the lateral forces exerted from the ground to the wheels, $\vec{v}_i\,(i=1,2)$ is the velocity of the robot center, and contact forces between the robot body and the cube are $\vec{N}_i\,(i=1,2)$.

In the present study, the Newton-Euler method is used to derive the equations of motion. Referring to Figure 2, the equations of motion for the first robot are obtained as follows:

$$\begin{aligned}&\sum F_x = ma_x\\&N_1\cos\theta + F_{L1}\cos\alpha_1 + F_{R1}\cos\alpha_1 - \lambda_1\sin\alpha_1 = m\ddot{x}_1\end{aligned} \tag{1}$$

$$\begin{aligned}&\sum F_y = ma_y\\&N_1\sin\theta + F_{L1}\sin\alpha_1 + F_{R1}\sin\alpha_1 + \lambda_1\cos\alpha_1 = m\ddot{y}_1\end{aligned} \tag{2}$$

$$\sum M_{c_1} = (F_{R_1} - F_{L_1})R_1 = I\ddot{\alpha}_1 \tag{3}$$

where m is the mass of the robots, $\ddot{\alpha}_1$ is the angular acceleration of the first robot, $\ddot{x}_1$ and $\ddot{y}_1$ are the horizontal and vertical accelerations of the first robot center of mass and I is the robots moment of inertia around their centers. By defining the following relation, we have:

$$N_1 = K\delta_1 + c\dot{\delta}_1 \tag{4}$$

where parameters K and c are the stiffness and damping coefficients of the cube, respectively.

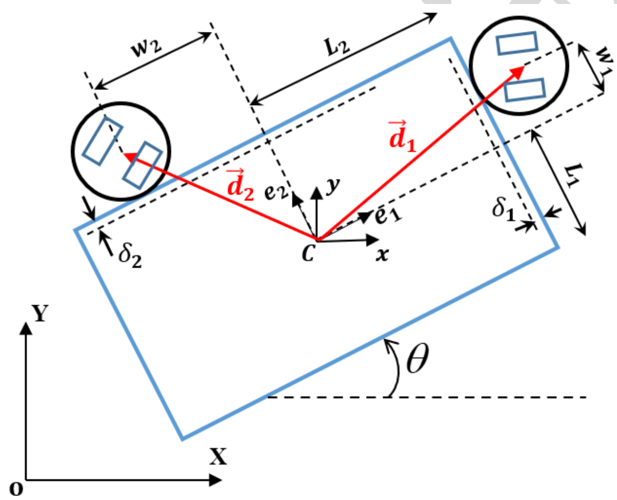

Figure 1. The schematic of the transporting system, including two cylindrical mobile robots collaborating to move a cube in grasping strategy.

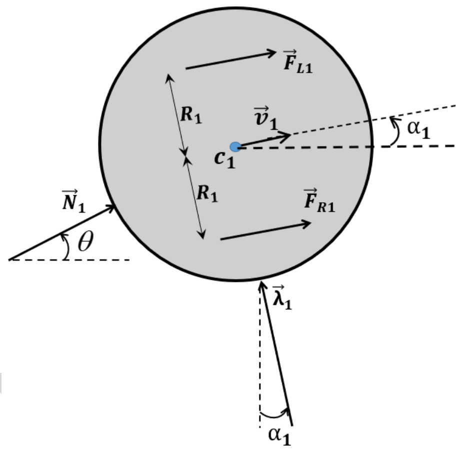

Figure 2. Free-body diagram of the first robot.

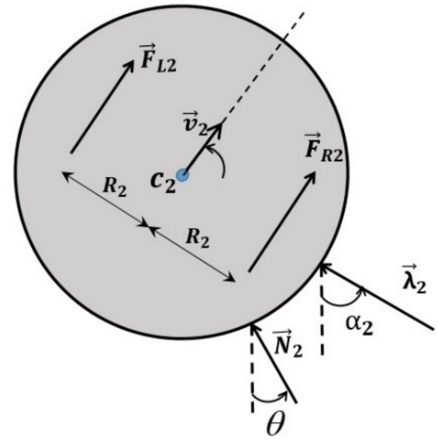

Figure 3. Free-body diagram of the second robot.

For the second robot, we have similarly:

$$\sum F_x = ma_x$$
$$-N_2 \sin\theta + F_{L2}\cos\alpha_2 + F_{R2}\cos\alpha_2 - \lambda_2 \sin\alpha_2 = m\ddot{x}_2 \tag{5}$$

$$\sum F_y = ma_y$$
$$N_2 \cos\theta + F_{L2}\sin\alpha_2 + F_{R2}\sin\alpha_2 + \lambda_2 \cos\alpha_2 = m\ddot{y}_2 \tag{6}$$

$$\sum M_{c_2} = (F_{R_2} - F_{L_2})R_2 = I\ddot{\alpha}_2 \tag{7}$$

and

$$N_2 = K\delta_2 + c\dot{\delta}_2 \tag{8}$$

where $\ddot{\alpha}_2$ is the angular acceleration of the second robot, $\ddot{x}_2$ and $\ddot{y}_2$ are the horizontal and vertical accelerations of the second robot center of mass, respectively.

2.2 Derivation of the dynamic equations of the cube

In Figure 4, the free-body diagram of the cube is presented. To derive the dynamic equations of the cube, according to the free-body diagram drawn in Figure 4 and using the Newton-Euler relations, we have:

$$\sum F_x = ma_x \rightarrow -N_1\cos\theta + N_2\sin\theta = M\,\ddot{x}_c \tag{9}$$

$$\sum F_y = ma_y \rightarrow -N_1\sin\theta - N_2\cos\theta = M\,\ddot{y}_c \tag{10}$$

$$\sum M_c = I_c\ddot{\theta} \rightarrow N_1 w_1 + N_2 w_2 = I_c\ddot{\theta} \tag{11}$$

where M is the mass of the cube, $\ddot{x}_c$ and $\ddot{y}_c$ are the horizontal and vertical accelerations of the cube, respectively, and I_c is the cube moment of inertia around its center.

2.3 Derivation of the kinematic equations of the robots

Considering Figure 1 and using the rotating coordinate system with the cube's angular velocity ω_s, the kinematic equations of the first robot are obtained as follows:

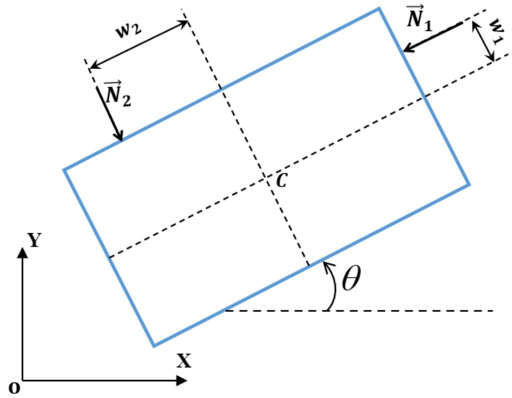

Figure 4. Free-body diagram of the cube.

$$x_1 \vec{i} + y_1 \vec{j} = x_c \vec{i} + y_c \vec{j} + \vec{d}_1 \tag{12}$$

$$\dot{x}_1 \vec{i} + \dot{y}_1 \vec{j} = \dot{x}_c \vec{i} + \dot{y}_c \vec{j} + \vec{v}_{rel} + \vec{\omega}_s \times \vec{d}_1 \tag{13}$$

$$\ddot{x}_1 \vec{i} + \ddot{y}_1 \vec{j} = \underbrace{\ddot{x}_c \vec{i} + \ddot{y}_c \vec{j}}_{a_0} + \underbrace{\ddot{w}_1 \vec{e}_2 - \ddot{\delta}_1 \vec{e}_1}_{a_{rel}} + \dot{\vec{\omega}}_s \times \vec{d}_1 + \vec{\omega}_s \times (\vec{\omega}_s \times \vec{d}_1) + 2\vec{\omega}_s \times \underbrace{\left[\dot{w}_1 \vec{e}_2 - \dot{\delta}_1 \vec{e}_1 \right]}_{v_{rel}} \tag{14}$$

where (x_1, y_1), $(\dot{x}_1, \dot{y}_1)$ and $(\ddot{x}_1, \ddot{y}_1)$ denote the position, velocity and acceleration components of the first robot center of mass, respectively. Moreover, (x_c, y_c), $(\dot{x}_c, \dot{y}_c)$ and $(\ddot{x}_c, \ddot{y}_c)$ denote the position, velocity and acceleration components of the cube center of mass, respectively. Based on Figure 1, vector $\vec{d}_1$ can be decomposed and rewritten as follows:

$$\vec{e}_1 = \cos\theta \vec{i} + \sin\theta \vec{j} \tag{15}$$

$$\vec{e}_2 = -\sin\theta \vec{i} + \cos\theta \vec{j} \tag{16}$$

$$\vec{d} = (L_2 + R - \delta_1)\vec{e}_1 \tag{17}$$

$$\vec{d}_1 = \vec{d} + w_1 \vec{e}_2 \rightarrow \vec{d}_1 = (L_2 + R - \delta_1)\vec{e}_1 + w_1 \vec{e}_2 \tag{18}$$

where R is the robot body radius.

Notice that the parameters R_1 and R_2 (See Figure 2 and Figure 3) are considered to be equal to the robot body radius, i.e. R. In other words, the robots' wheels and consequently the forces $\vec{F}_{Li}$ and $\vec{F}_{Ri}$ are tangent to the cylindrical body of the robots.

Similarly, for the second robot, we have:

$$x_2 \vec{i} + y_2 \vec{j} = x_c \vec{i} + y_c \vec{j} + \vec{d}_2 \tag{19}$$

$$\dot{x}_2 \vec{i} + \dot{y}_2 \vec{j} = \dot{x}_c \vec{i} + \dot{y}_c \vec{j} + \vec{v}_{rel} + \vec{\omega}_s \times \vec{d}_2 \tag{20}$$

$$\ddot{x}_2 \vec{i} + \ddot{y}_2 \vec{j} = \underbrace{\ddot{x}_c \vec{i} + \ddot{y}_c \vec{j}}_{a_0} \underbrace{- \ddot{w}_2 \vec{e}_1 - \ddot{\delta}_2 \vec{e}_2}_{a_{rel}} + \dot{\vec{\omega}}_s \times \vec{d}_2 + \vec{\omega}_s \times (\vec{\omega}_s \times \vec{d}_2) + 2\vec{\omega}_s \times \underbrace{\left[-\dot{w}_2 \vec{e}_1 - \dot{\delta}_2 \vec{e}_2 \right]}_{v_{rel}} \tag{21}$$

$$\vec{d}_2 = (L_1 + R - \delta_2)\vec{e}_2 - w_2 \vec{e}_1 \tag{22}$$

where $(x_2, y_2), (\dot{x}_2, \dot{y}_2)$ and $(\ddot{x}_2, \ddot{y}_2)$ denote the position, velocity and acceleration components of the second robot center of mass, respectively.

2.4 Non-holonomic constraints

To derive the non-holonomic constraints of the robots, the following steps are taken:

$$(\dot{x}_i \vec{i} + \dot{y}_i \vec{j}).\vec{e}_n = 0, \; \vec{e}_n = -\sin(\alpha_i)\vec{i} + \cos(\alpha_i)\vec{j}, \quad i = 1,2 \tag{23}$$

$$\underbrace{\begin{bmatrix} -\sin(\alpha_i) & \cos(\alpha_i) \end{bmatrix}}_{A_i(\alpha_i)} \begin{bmatrix} \dot{x} \\ \dot{y} \end{bmatrix}_i = 0 \quad \rightarrow \quad A_i(\alpha_i) \begin{bmatrix} \dot{x} \\ \dot{y} \end{bmatrix}_i = 0, \qquad i = 1,2 \tag{24}$$

By differentiating equation (24) with respect to time, we have:

$$\dot{A}_i(\alpha_i) \begin{bmatrix} \dot{x} \\ \dot{y} \end{bmatrix}_i + A_i(\alpha_i) \begin{bmatrix} \ddot{x} \\ \ddot{y} \end{bmatrix}_i = 0, \qquad i = 1,2 \tag{25}$$

2.5 Solving equations

The vector of unknowns that are used for dynamic modeling, is defined as

$$\chi = \begin{bmatrix} \ddot{\delta}_1 & \ddot{\delta}_2 & \ddot{w}_1 & \ddot{w}_2 & \lambda_1 & \lambda_2 \end{bmatrix}^T \tag{26}$$

which can be obtained through the following relation:

$$\chi = -A_L^{-1} B_L \tag{27}$$

where,

$$A_L = \begin{bmatrix} -\cos\theta & 0 & -\sin\theta & 0 & \frac{\sin\alpha_1}{m} & 0 \\ -\sin\theta & 0 & \cos\theta & 0 & \frac{-\cos\alpha_1}{m} & 0 \\ 0 & \sin\theta & 0 & -\cos\theta & 0 & \frac{\sin\alpha_2}{m} \\ 0 & -\cos\theta & 0 & -\sin\theta & 0 & \frac{-\cos\alpha_2}{m} \\ 0 & 0 & 0 & 0 & \frac{1}{m} & 0 \\ 0 & 0 & 0 & 0 & 0 & \frac{1}{m} \end{bmatrix} \tag{28}$$

$$B_L = \begin{bmatrix} b_{1,1} & b_{2,1} & b_{3,1} & b_{4,1} & b_{5,1} & b_{6,1} \end{bmatrix}^T \tag{29}$$

$$b_{1,1}=\frac{N_2.\sin\theta}{M}-2\dot{\theta}\left(\dot{w}_1\cos\theta-\dot{\delta}_1\sin\theta\right)-\frac{1}{m}((F_{L1}+F_{R1}).\cos\alpha_1+N_1.\cos\theta)$$
$$-\dot{\theta}^2(A.\cos\theta-w_1\sin\theta)-\frac{N_1.\cos\theta}{M}-\frac{1}{I_c}(w_1N_1+w_2N_2)(A.\sin\theta+w_1\cos\theta) \tag{30}$$

$$b_{2,1}=\frac{-N_2.\cos\theta}{M}-2\dot{\theta}\left(\dot{w}_1\sin\theta+\dot{\delta}_1\cos\theta\right)-\frac{1}{m}((F_{L1}+F_{R1}).\sin\alpha_1+N_1.\sin\theta)$$
$$-\dot{\theta}^2(A.\sin\theta+w_1\cos\theta)-\frac{N_1.\sin\theta}{M}+\frac{1}{I_c}(w_1N_1+w_2N_2)(A.\cos\theta-w_1\sin\theta) \tag{31}$$

$$b_{3,1}=\frac{N_2.\sin\theta}{M}+2\dot{\theta}\left(\dot{w}_2\sin\theta+\dot{\delta}_2\cos\theta\right)-\frac{1}{m}((F_{L2}+F_{R2}).\cos\alpha_2-N_2.\sin\theta)$$
$$+\dot{\theta}^2(B.\sin\theta+w_2\cos\theta)-\frac{N_1.\cos\theta}{M}-\frac{1}{I_c}(w_1N_1+w_2N_2)(B.\cos\theta-w_2\sin\theta) \tag{32}$$

$$b_{4,1}=\frac{-N_1.\sin\theta}{M}-2\dot{\theta}\left(\dot{w}_2\cos\theta-\dot{\delta}_2\sin\theta\right)-\frac{1}{m}((F_{L2}+F_{R2}).\sin\alpha_2+N_2.\cos\theta)-\dot{\theta}^2(B.\cos\theta-w_2\sin\theta)$$
$$-\frac{N_2.\cos\theta}{M}-\frac{1}{I_c}(w_1N_1+w_2N_2)(B.\sin\theta+w_2\cos\theta) \tag{33}$$

$$b_{5,1}=-\frac{1}{m}\left[N_1\sin\left(\alpha_1-\theta\right)+m\dot{x}_1\dot{\alpha}_1\cos\alpha_1+m\dot{y}_1\dot{\alpha}_1\sin\alpha_1\right] \tag{34}$$

$$b_{6,1}=\frac{1}{m}\left[N_2\cos\left(\alpha_2-\theta\right)-m\dot{x}_2\dot{\alpha}_2\cos\alpha_2-m\dot{y}_2\dot{\alpha}_2\sin\alpha_2\right] \tag{35}$$

$$\lambda_1=m\dot{x}_1\dot{\alpha}_1\cos\alpha_1+m\dot{y}_1\dot{\alpha}_1\sin\alpha_1+N_1\sin\left(\alpha_1-\theta\right) \tag{36}$$

$$\lambda_2=m\dot{x}_2\dot{\alpha}_2\cos\alpha_2+m\dot{y}_2\dot{\alpha}_2\sin\alpha_2-N_2\cos\left(\alpha_2-\theta\right) \tag{37}$$

$$\begin{aligned} N_1&=K\delta_1+C.\dot{\delta}_1, \qquad & A&=R+\frac{L}{2}-\delta_1\\ N_2&=K\delta_2+C.\dot{\delta}_2, \qquad & B&=R+\frac{L}{4}-\delta_2 \end{aligned} \tag{38}$$

$$\ddot{\alpha}_1=\frac{(F_{R1}-F_{L1})R_1}{I},\ \ddot{\alpha}_2=\frac{(F_{R2}-F_{L2})R_2}{I} \tag{39}$$

where L is the length of the cube which is considered as twice its width.

3. Cooperative control strategy

In the present study, MPC is used where physical constraints such as actuator saturation, can also be considered. By correctly tuning the controller's parameters and adjusting the weighting coefficients of the cost function, in addition to satisfying the constraints, a compromise can be reached between the defined objectives (such as path tracking error and control effort).

3.1 Model predictive control

The structure of model predictive control is divided into the following three main parts:

1. Using the model to predict the future behavior of the system.
2. Calculating the optimal control signal by optimizing the objective function.
3. Using the receding horizon approach and applying the first control signal to the system.

State vector of the system is considered as

$$X=[x_c \quad y_c \quad \theta \quad w_1 \quad w_2 \quad \alpha_1 \quad \alpha_2 \quad \delta_1 \quad \delta_2 \quad \dot{x}_c \quad \dot{y}_c \quad \dot{\theta} \quad \dot{w}_1 \quad \dot{w}_2 \quad \dot{\alpha}_1 \quad \dot{\alpha}_2 \quad \dot{\delta}_1 \quad \dot{\delta}_2]^T \tag{40}$$

The cost function which should be minimized is defined as follows

$$J=\sum_{i=k}^{k+N_p}\left[\gamma_1 e_x^T(i)R_e e_x(i)+\gamma_2 e_w^T(i)e_w(i)+\gamma_3 e_v^T(i)e_v(i)+\gamma_4 e_{\dot{\alpha}}^T(i)e_{\dot{\alpha}}(i)+\gamma_5\tau^T(i)\tau(i)\right] \tag{41}$$

where,

$$\begin{aligned}
&e_x=X(1:3)-X_r(1:3)=\begin{bmatrix}x_c\\ y_c\\ \theta\end{bmatrix}-\begin{bmatrix}x_r\\ y_r\\ \theta_r\end{bmatrix},\\
&e_w=X(4:5)=\begin{bmatrix}w_1\\ w_2\end{bmatrix},\\
&e_v=X(10:12)-X_r(10:12)=\begin{bmatrix}\dot{x}_c\\ \dot{y}_c\\ \dot{\theta}\end{bmatrix}-\begin{bmatrix}\dot{x}_r\\ \dot{y}_r\\ \dot{\theta}_r\end{bmatrix}\\
&e_{\dot{\alpha}}=X(15:16)-X_r(15:16)=\begin{bmatrix}\dot{\alpha}_1\\ \dot{\alpha}_2\end{bmatrix},\\
&\tau=\begin{bmatrix}F_{R_1} & F_{L_1} & F_{R_2} & F_{L_2}\end{bmatrix}^T,
\end{aligned} \tag{42}$$

in which, k is the current time index and γ_i are weighting coefficients. The weighting coefficients $\gamma_1,\gamma_2,\gamma_3,\gamma_4,\gamma_5$ and R_e were selected through iterative trial-and-error with the following rationale:

1-Increasing γ_1 and diagonal terms of R_e will prioritize the cost of position and yaw tracking errors.

2- Increasing γ_2 will force w_1 and w_2 to converge to zero.

3- Increasing γ_3 moderate weight to avoid aggressive acceleration.

4- Increasing γ_4 prevents fast angular velocity of robots.

5- Increasing γ_4 decreases the control effort.

The cost function should be minimized subject to the following constraints:

$$\begin{aligned}
&\left|F_{R_1}\right|<F_{1,\max},\left|F_{L_1}\right|<F_{1,\max},\\
&\left|F_{R_2}\right|<F_{2,\max},\left|F_{L_2}\right|<F_{2,\max},\\
&\left|w_1\right|<\frac{3}{4}L_1,\left|w_2\right|<\frac{3}{4}L_2
\end{aligned} \tag{43}$$

4. Simulation and results

In Table 1, the required parameters for the system simulation are presented. For doing the simulation, an initial state vector is considered as

$$X(0) = [2m \quad 0 \quad 0.5rad \quad 0 \quad 0 \quad 0 \quad 0 \quad 0 \quad 0. \quad 0 \quad 0 \quad 0 \quad 0 \quad 0 \quad 0 \quad 0 \quad 0 \quad 0]^T \tag{44}$$

, and reference state vector is

$$X_r = 0_{18\times 1} \tag{45}$$

, and other parameters are

$$R_e = \begin{bmatrix} 1 & 0 & 0 \\ 0 & 1 & 0 \\ 0 & 0 & 10 \end{bmatrix},\ \gamma_1 = 500,\ \gamma_2 = 50,\ \gamma_3 = 50,\ \gamma_4 = 0.1,\ \gamma_5 = 0.02. \tag{46}$$

The implementation software and MPC discretization characteristics are:

- Optimization solver**:** MATLAB® fmincon with sequential quadratic programming (SQP).
- Model discretization**:** Zero-order hold with sampling time $\Delta T = 0.05s$ using forward Euler method.

Figure 5 illustrates the cooperative transportation sequence at eight-time instants (t=0.05, 0.45, 1, 1.2, 1.9, 2.4, 3, 3.4, 3.5). At t=0 s, the cube and two robots start from arbitrary initial positions. Between t=0~3s, the cube undergoes coordinated translation and rotation as the robots apply optimal control forces under nonholonomic and contact constraints.

Table 1. Simulation, Control, Geometrical and Physical Parameters.

Parameter	Description	Value
T_f	Simulation Time	4 s
ΔT	Time Step	0.05 s
N_p	Prediction Horizon	4
N_c	Control Horizon	4
$F_{1,\max}$, $F_{2,\max}$	Actuator Force Bound	4 N
K	Stiffness Coefficient	400 N/m
C	Damping Coefficient of Cube	15 N.s/m
m_1, m_2	Mass of Robots	0.2 kg
M	Mass of Cube	4 kg
I_c	Cube Moment of Inertia	1 kg.m^2
R	Radius of Robots	0.15 m
L	Length of Cube	2 m

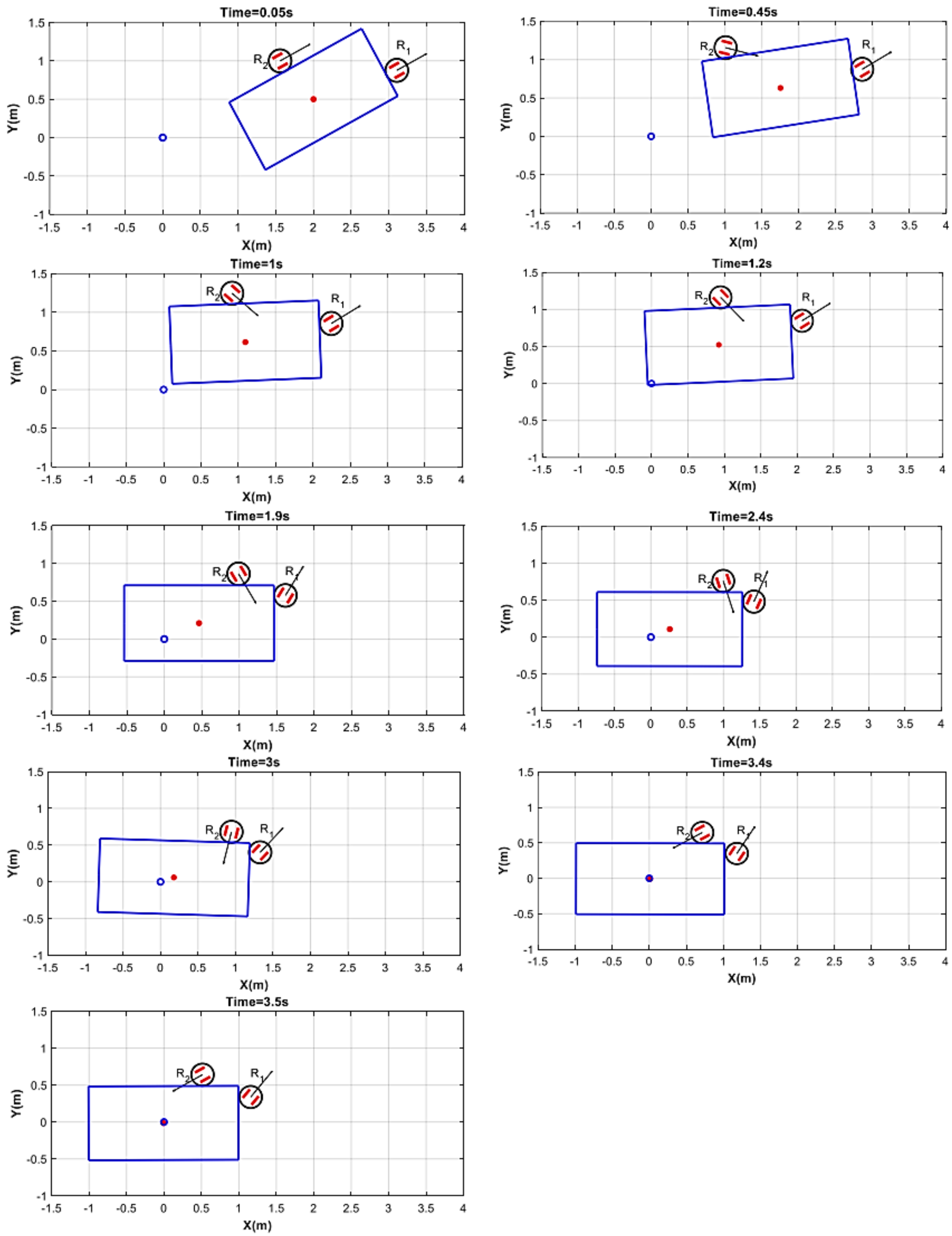

Figure 5. Sequential snapshots of the cooperative transportation process at eight-time instants (t=0.05,0.45,1,1.2,1.9,2.4,3, 3.4,3.5), showing the positions and orientations of the cube and two nonholonomic mobile robots (circles) under the proposed full multibody dynamic MPC framework. The cube successfully moves from its initial configuration (Slot 1) to the desired destination (Slot 9).

By t=3~3.5 s, the cube approaches the desired pose with decreasing tracking error. At t=3.5s, the cube successfully reaches the target configuration while both robots maintain stable contact. The sequence demonstrates that two nonholonomic robots are sufficient for dynamic cooperative transport using the proposed full multibody dynamic MPC framework. The cube position and its yaw angle are illustrated in Figure 6 and Figure 7, respectively. It is clear that, two robots have successfully cooperated to move the cube from the starting point to the desired destination in the presence of constraints.

Figure 8 shows the time history of reaction forces between the two robots and the cube. It is evident that the connection and interaction between the two robots and the cube during the movement are reasonable. The control forces (the force of the left and right wheels) of two robots, as well as the difference between them are illustrated in Figure 9 and Figure 10. By the suitable control logic, the actuator saturation ([-4N, 4N]) is satisfied. The difference between the F_R and F_L will result in angular acceleration for each robot ($\ddot{\alpha}_i$).

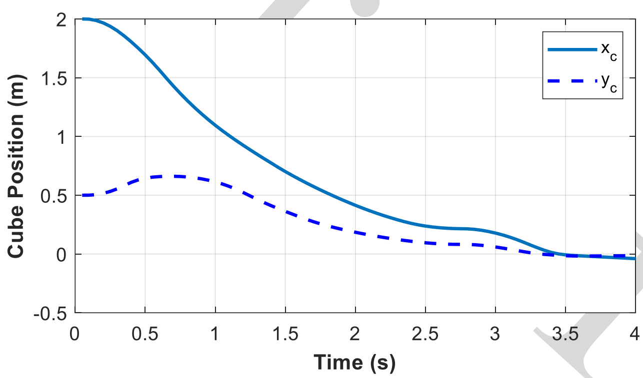

Figure 6. Cube position from the initial to the desired destination.

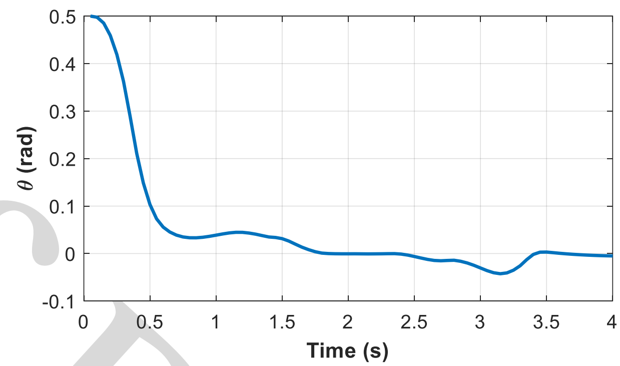

Figure 7. Cube yaw angle with respect to time during its movement from the initial to the desired destination.

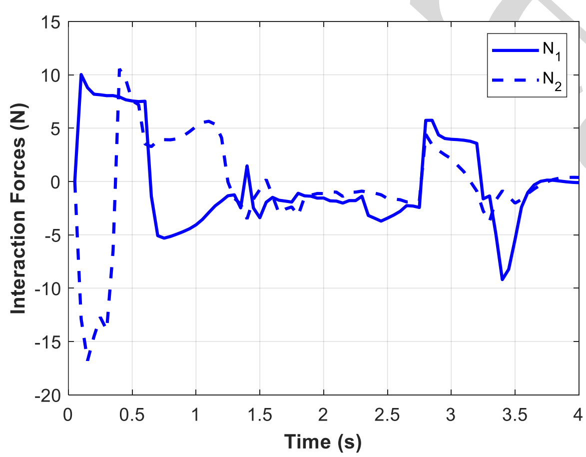

Figure 8. The diagram of reaction forces between the two robots and the cube with respect to time during the movement from the start to the desired destination.

Figure 11 shows the lateral forces exerted by the ground on the wheels of the robots. As observed, these forces are bounded and applied by the ground to the wheels of the robots throughout the entire cube movement period. The variation in the relative distances between robots' centers and cube along the rectangle sides (w_1 and w_2) is illustrated in Figure 12. It can be concluded that by control logic robots remain in the desired area along the rectangular cube, in other words robots do not escape from the cube.

Furthermore, Figure 13 shows the variations in robots' penetration into the cube (δ_1 and δ_2) from the start to the desired destination.

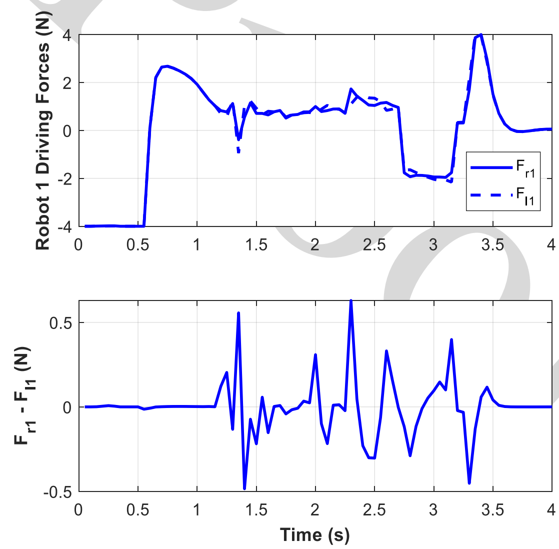

Figure 9. The first robot wheels' driving forces generated by control logic.

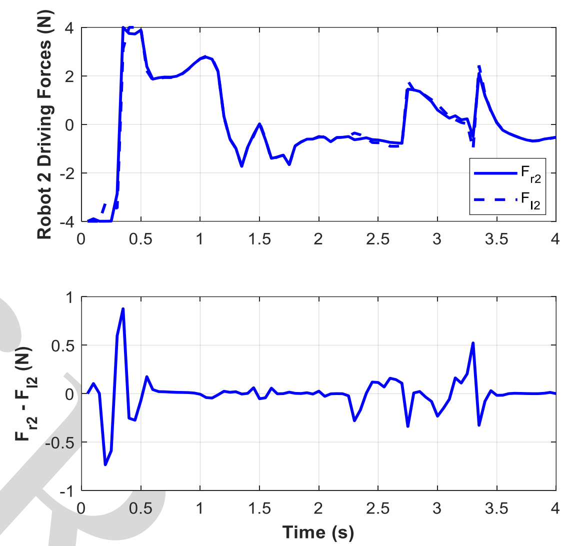

Figure 10. The second robot wheels' driving forces generated by control logic.

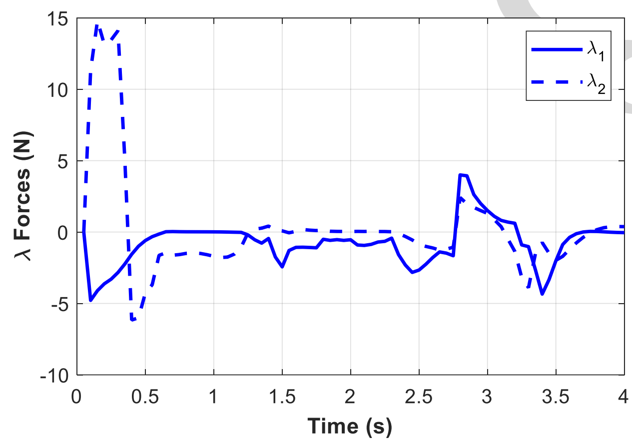

Figure 11. Forces exerted by the ground on the wheels of the robots.

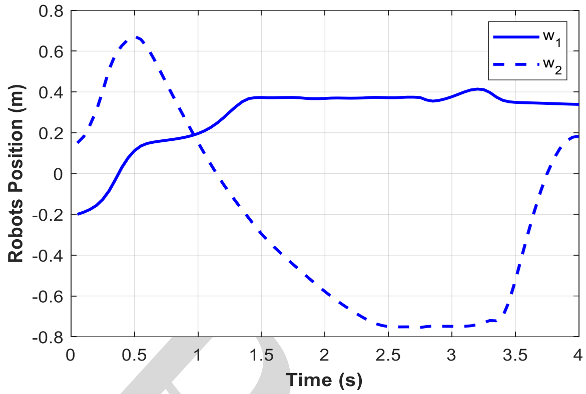

Figure 12. Variation in the relative distances between robots' centers and cube along the rectangle sides.

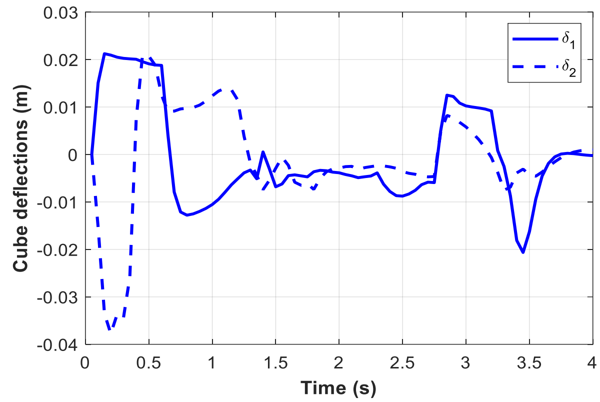

Figure 13. Robots' penetration into the cube.

5. Discussion

The simulation results presented in Section 4 demonstrate that the proposed full multibody dynamic MPC framework successfully enables two nonholonomic mobile robots to cooperatively transport a rigid cube from an arbitrary initial configuration to a desired pose while satisfying all system constraints. This section interprets these results, compares them with related work, and discusses limitations and future directions.

5.1 Interpretation of Key Results

Successful transportation with only two robots: Figure 6 and Figure 7 show that the cube's position and yaw angle converge smoothly to their desired values within the 4 s simulation horizon. This confirms that, within the scope of the simulated scenarios, two nonholonomic robots are sufficient for stable cooperative transport when full dynamics and contact constraints are explicitly considered in the MPC formulation. This finding is significant because most existing cooperative transport studies require three or more robots [7, 8] or rely on omnidirectional/holonomic platforms [10] to achieve similar maneuverability.

Constraint satisfaction: Figure 9 and Figure 10 confirm that actuator forces remain within the prescribed $[-4\text{ N}, 4\text{ N}]$ saturation limits, demonstrating the MPC's ability to enforce physical feasibility. Figure 11 shows that lateral ground forces on the wheels remain bounded, indicating stable nonholonomic motion without slip. Figure 12. And Figure 13 show that the relative distances between robots and the cube (w_i) and penetrations (δ_i) remain within acceptable bounds, confirming that contact maintenance constraints successfully prevent robot detachment – a critical requirement for grasping-based transport.

Dynamic effects during maneuvers: The reaction forces shown in Figure 8 exhibit transient peaks during the initial acceleration and turning phases (approximately $t = 0$–1 s). These peaks would be entirely neglected by quasi-static or kinematic-only approaches [5, 18]. Their presence in our results validates the necessity of full multibody dynamics for aggressive or high-speed maneuvers.

Table 2. Comparison with Related Work.

Criterion	Quasi-static/Kinematic Approaches e.g., [5, 18]	Distributed MPC [10]	Learning-based [20]	**This Work**
Inertial effects	× Neglected	√ Included (multibody)	× Largely kinematic	√ Full multibody dynamics
Nonholonomic constraints	× Often simplified	√ Yes	× Not explicitly	√ Explicitly enforced
Contact constraints	× Implicit/assumed	√ Yes	× Not addressed	√ Explicit contact maintenance
Number of robots	≥ 3	≥ 3	2	2 (minimal)
MPC framework	× Not used	√ Distributed	× DDPG (RL)	√ Centralized MPC
Suitable for fast maneuvers	× No	√ Yes	× Limited	√ Yes

5.2 Comparison with Related Work.

Key differences from [10]: While Ebel and Eberhard used distributed MPC with omnidirectional robots and communication between neighbors, our approach uses centralized MPC with nonholonomic differential-drive robots and explicitly enforces contact maintenance constraints – a critical feature for grasping-based transport that is absent in pushing-only strategies.

Key differences from [20]: Tang et al. employed DDPG-based navigation for dual-robot formation transport, but their model is largely kinematic and does not incorporate multibody dynamics or contact forces. Our MPC framework offers constraint satisfaction and physical fidelity that are advantageous for dynamic maneuvers, although a direct quantitative comparison with these methods remains as future work.

5.3 Limitations

Despite the promising results, several limitations should be acknowledged:

1. Simulation-only validation: The results are based on numerical simulations. Experimental validation with physical robots is necessary to assess real-world challenges such as sensor noise, communication delays, and unmodeled friction.
2. Planar assumption: The model assumes motion in a planar environment. Extension to three-dimensional terrains with slopes or uneven surfaces would require additional considerations for stability and contact modeling.
3. Object shape: The simulations used a cube. While the formulation is general, performance for highly irregular or non-convex objects may require additional constraints or formation reconfiguration strategies.
4. Computational load: MPC with full multibody dynamics can be computationally intensive. Real-time implementation may require optimization techniques such as shorter horizons or code generation.

5.4 Computational cost and real-time feasibility

The computational cost of the proposed MPC scheme was evaluated on a standard desktop computer (Intel Core i7, 16 GB RAM) using MATLAB® fmincon with SQP algorithm. The average solve time per iteration is approximately 1.5 s, which exceeds the 0.05 s sampling interval. Therefore, real-time implementation on this hardware configuration is not currently feasible. This limitation arises primarily from the use of a general-purpose optimization solver in an interpreted environment. However, several established strategies can address this issue for practical deployment: (1) implementation in compiled languages such as C++ with tailored QP solvers (e.g., qpOASES, OSQP, or FORCES Pro), which typically achieve solve times two to three orders of magnitude faster; (2) reduction of the prediction horizon or problem size; (3) exploitation of the problem's sparse structure; or (4) use of more powerful embedded hardware such as FPGA-based platforms. These improvements are identified as essential steps toward real-time implementation and are considered in the future work section.

5.5 Future Directions

Building on the contributions of this work, several avenues for future research are identified:

- **Experimental validation:** Implement the proposed MPC framework on physical differential-drive robots (e.g., Pioneer P3-DX or e-puck platforms) to validate simulation findings.
- **Obstacle avoidance:** Integrate obstacle avoidance constraints into the MPC formulation for operation in cluttered environments.
- **Robust MPC:** Extend the framework to handle model uncertainties (e.g., unknown object mass, friction coefficients) using robust or adaptive MPC techniques.
- **Heterogeneous robot teams:** Explore cooperative transport using mixed teams of nonholonomic and holonomic robots to combine maneuverability with payload capacity.

6. Conclusions

This paper has presented a Model Predictive Control (MPC) framework for cooperative transportation of a rigid body using only two nonholonomic mobile robots – the minimal configuration capable of manipulating an object in the plane. The key contribution is the integration of a full multibody dynamic model within a centralized MPC formulation, which explicitly accounts for inertial coupling, nonholonomic constraints, and physical contact interactions between robots and object. Unlike prior approaches that rely on quasi-static or kinematic approximations – which neglect inertial effects– our method provides a physically accurate representation essential for dynamic manipulation tasks.

The MPC controller was designed to simultaneously enforce three critical constraint sets: (1) nonholonomic motion constraints of differential-drive robots, (2) actuator saturation limits, and (3) explicit contact maintenance constraints that prevent robot detachment from the object boundary. Numerical simulations validated the controller's effectiveness in transporting objects from arbitrary initial configurations to desired poses while maintaining all constraints. It is important to emphasize, however, that these results are obtained under simulation and nominal operating conditions; experimental validation under real-world disturbances and uncertainties has not yet been performed. Notably, the results demonstrate that, for the scenarios tested in this study, only two nonholonomic robots are sufficient for stable transportation when leveraging this dynamic, aware control approach, a finding that challenges the conventional wisdom that three or more robots are required for robust cooperative transport. A formal proof of minimality, however, would require further theoretical investigation.

The proposed framework contributes to the literature by providing a methodologically complete solution that combines full multibody dynamics with constrained optimal control for minimal-robot configurations. While the comparisons with existing methods are primarily qualitative, they highlight the potential advantages of the proposed approach in terms of physical fidelity and constraint satisfaction.

Future work will focus on three main directions. First, experimental validation using physical differential-drive robots is essential to assess the framework's performance under real-world conditions. Second, robustness analysis against parameter uncertainties, external disturbances, and modeling errors will be conducted to extend the controller's applicability to more challenging environments. Third, the scalability of the approach to larger robot teams will be investigated, exploring both centralized and distributed MPC formulations. These extensions will further strengthen the practical relevance of the proposed framework.

Disclosure statement

No potential conflict of interest was reported by the author(s).

Notes on contributors

Zahra Shirmohammadi Esfeh received her B.Sc. degree in Mechanical Engineering from Ayatollah Borujerdi University, Borujerd, Iran, in 2019. She received her M.Sc. degree in Mechanical Engineering from the University of Guilan, Rasht, Iran, in 2024. Her research interests include robotics, cooperative mobile robots, transportation, and model predictive control (MPC).

Hamed Kouhi was born in Guilan, Iran, in 1986. He received a B.S. degree in mechanical engineering from the University of Guilan in 2008 and, in 2010, he received his M.S. degree in mechanical engineering from Sharif University of Technology, Tehran, Iran, on the topic of the "Control of Car-Like Multi Robot for Following and Hunting a Moving Target". He received his PhD degree, in mechanical engineering, from Amirkabir University of Technology, Tehran, Iran, in 2017, on the topic of Spacecraft Dynamics and Control. He is now Assistant Professor at the University of Guilan and his current research interests include: control, autonomous vehicles, model predictive control, navigation, multi agent system, system identification and dynamics.

Behnam Miripour Fard is an Associate Professor in the Faculty of Mechanical Engineering at the University of Guilan, Iran. He previously held faculty positions at Hamedan University of Technology, serving as the Head of the Department of Robotics Engineering. He earned his B.Sc. in Mechanical Engineering from the University of Guilan in 2005, followed by an M.Eng. from Bu-Ali Sina University in 2008, specializing in the dynamic stability of humanoid systems. He completed his Ph.D. in Mechanical Engineering at the University of Guilan in 2013, focusing on human-inspired motion generation and the control of bipedal robots under external perturbations. During his doctoral studies, he was a Visiting Ph.D. Student at the Robotics Institute of Carnegie Mellon University (CMU). His current research interests lie at the forefront of robotics and autonomous systems, integrating machine learning and robust Model Predictive Control (MPC) to address complex challenges in bipedal locomotion, the biomechanics of walking, and the navigation of autonomous vehicles.

Esmaeil Salahshoor is an Assistant Professor of Mechanical Engineering at Islamic Azad University of Izeh with research interests in Multibody System Dynamics. He received his B.Sc. from the University of Guilan in 2007 and his M.Sc. from BuAliSina University in 2009 and his Ph.D. from Yazd University in 2018 in Mechanical Engineering. His research is concerned with clearance joint in mechanisms, robotics, multibody system dynamics and optimization.

References

[1] H. Sayyaadi, H. Kouhi, and H. Salarieh, "Control of car-like (wheeled) multi robots for following and hunting a moving target," *Scientia Iranica,* vol. 18, no. 4, pp. 950-965, 2011.

[2] E. Tuci, M. H. Alkilabi, and O. Akanyeti, "Cooperative object transport in multi-robot systems: A review of the state-of-the-art," *Frontiers in Robotics and AI,* vol. 5, p. 59, 2018.

[3] C. R. Kube and H. Zhang, "Collective robotics: From social insects to robots," *Adaptive behavior,* vol. 2, no. 2, pp. 189-218, 1993.

[4] B. P. Gerkey and M. J. Mataric, "Pusher-watcher: An approach to fault-tolerant tightly-coupled robot coordination," in *Proceedings 2002 IEEE International Conference on Robotics and Automation (Cat. No. 02CH37292)*, 2002, vol. 1: IEEE, pp. 464-469.

[5] Y. Wang and C. W. de Silva, "Cooperative transportation by multiple robots with machine learning," in *2006 IEEE international conference on evolutionary computation*, 2006: IEEE, pp. 3050-3056.

[6] J. Sasaki, J. Ota, E. Yoshida, D. Kurabayashi, and T. Arai, "Cooperating grasping of a large object by multiple mobile robots," in *Proceedings of 1995 IEEE International Conference on Robotics and Automation*, 1995, vol. 1: IEEE, pp. 1205-1210.

[7] Z. Wang and M. Schwager, "Kinematic multi-robot manipulation with no communication using force feedback," in *2016 IEEE international conference on robotics and automation (ICRA)*, 2016: IEEE, pp. 427-432.

[8] G. A. Pereira[1], V. Kumar[1], and M. F. Campos, "Decentralized algorithms for multirobot manipulation via caging," *Algorithmic Foundations of Robotics V,* vol. 7, p. 257, 2003.

[9] T. Recker, M. Heinrich, and A. Raatz, "A comparison of different approaches for formation control of nonholonomic mobile robots regarding object transport," *Procedia CIRP,* vol. 96, pp. 248-253, 2021.

[10] H. Ebel and P. Eberhard, "Distributed decision making and control for cooperative transportation using mobile robots," in *International Conference on Swarm Intelligence*, 2018: Springer, pp. 89-101.

[11] C. C. Loh and A. Traechtler, "Cooperative transportation of aload using nonholonomic mobile robots," *Procedia Engineering,* vol. 41, pp. 860-866, 2012.

[12] X. Yang, K. Watanabe*, K. Izumi, and K. Kiguchi, "A decentralized control system for cooperative transportation by multiple non-holonomic mobile robots," *International Journal of Control,* vol. 77, no. 10, pp. 949-963, 2004.

[13] D. J. Stilwell and J. S. Bay, "Toward the development of a material transport system using swarms of ant-like robots," in *[1993] Proceedings IEEE International Conference on Robotics and Automation*, 1993: IEEE, pp. 766-771.

[14] H. W. Agung, "Advancements in cooperative mobile robots control strategies for large-scale material transport," *Kinetik: Game Technology, Information System, Computer Network, Computing, Electronics, and Control,* 2024.

[15] B. Hichri, J.-C. Fauroux, L. Adouane, I. Doroftei, and Y. Mezouar, "Design of cooperative mobile robots for co-manipulation and transportation tasks," *Robotics and computer-integrated manufacturing,* vol. 57, pp. 412-421, 2019.

[16] A. Yamashita, T. Arai, J. Ota, and H. Asama, "Motion planning of multiple mobile robots for cooperative manipulation and transportation," *IEEE Transactions on Robotics and Automation,* vol. 19, no. 2, pp. 223-237, 2003.

[17] L. Bruzzone, S. E. Nodehi, and P. Fanghella, "Tracked locomotion systems for ground mobile robots: A review," *Machines,* vol. 10, no. 8, p. 648, 2022.

[18] J. Chen, M. Gauci, W. Li, A. Kolling, and R. Groß, "Occlusion-based cooperative transport with a swarm of miniature mobile robots," *IEEE Transactions on Robotics,* vol. 31, no. 2, pp. 307-321, 2015.

[19] A. Yufka and M. Ozkan, "Formation-based cooperative transportation by a group of non-holonomic mobile robots," *International Journal of Advanced Robotic Systems,* vol. 12, no. 9, p. 120, 2015.

[20] L. Tang, R. Ma, B. Chen, and Y. Niu, "Dual-robot formation transport in random environment and narrow restricted area via improved DDPG navigation," *Discover Applied Sciences,* vol. 7, no. 3, p. 146, 2025.

[21] J. C. Tejada *et al.*, "Enhancing Object Manipulation and Transportation in Multi-Robot Systems with Soft Gripper Integration and Caging-Based Control," *Journal of Intelligent & Robotic Systems,* vol. 111, no. 3, p. 76, 2025.

[22] H. Ebel, M. Rosenfelder, and P. Eberhard, "Cooperative object transportation with differential-drive mobile robots: Control and experimentation," *Robotics and Autonomous Systems,* vol. 173, p. 104612, 2024.

[23] K. Haninger, K. Samuel, F. Rozzi, S. Oh, and L. Roveda, "Differentiable compliant contact primitives for estimation and model predictive control," in *2024 IEEE International Conference on Robotics and Automation (ICRA)*, 2024: IEEE, pp. 17146-17152.

[24] H. Zheng, X. Zhai, H. Wu, J. Pan, Z. Xu, and X. Zhou, "Interaction model estimation-based robotic force-position coordinated optimization for rigid–soft heterogeneous contact tasks," *Biomimetic Intelligence and Robotics,* vol. 5, no. 1, p. 100194, 2025.